A −1 ribosomal frameshift element that requires base pairing across four kilobases suggests a mechanism of regulating ribosome and replicase traffic on a viral RNA

Jennifer K. Barry* and W. Allen Miller†

Plant Pathology Department, Iowa State University, Ames, IA 50011

Edited by Reed B. Wickner, National Institutes of Health, Bethesda, MD, and approved June 14, 2002 (received for review April 12, 2002)

Programmed −1 ribosomal frameshifting is necessary for translation of the polymerase genes of many viruses. In addition to the consensus elements in the mRNA around the frameshift site, we found previously that frameshifting on *Barley yellow dwarf virus* RNA requires viral sequence located four kilobases downstream. By using dual luciferase reporter constructs, we now show that a predicted loop in the far downstream frameshift element must base pair to a bulge in a bulged stem loop adjacent to the frameshift site. Introduction of either two or six base mismatches in either the bulge or the far downstream loop abolished frameshifting, whereas mutations in both sites that restored base pairing reestablished frameshifting. Likewise, disruption of this base pairing abolished viral RNA replication in plant cells, and restoration of base pairing completely reestablished virus replication. We propose a model in which *Barley yellow dwarf virus* uses this and another long-distance base-pairing event required for cap-independent translation to allow the replicase copying from the 3′ end to shut off translation of upstream ORFs and free the RNA of ribosomes to allow unimpeded replication. This would be a means of solving the ''problem,'' common to positive strand RNA viruses, of competition between ribosomes and replicase for the same RNA template.

To encode proteins and regulate gene expression with minimal sequence, the mRNAs of many viruses harbor overlapping genes and induce the ribosome to change reading frame during translation (1, 2). In −1 frameshifting, a small percentage of the ribosomes back up one base relative to the codons in the initial reading frame (the zero frame) and continue elongation in the new (−1) frame. This process is facilitated by specific sequences and structures in the mRNA (3, 4). The known frameshift-inducing elements include the shifty (slippery) heptanucleotide at which the ribosome shifts frames, usually fitting the consensus: X XXY YYZ, where spaces separate codons in the zero frame, X is any base, Y is A or U, and Z is not G (2, 5), and a highly structured element beginning five to six bases downstream. This adjacent downstream element is usually a pseudoknot (4, 6). In some contexts, a simple stem loop may suffice (7, 8), but those exceptions may still require a pseudoknot for full frameshift stimulation (9).

The mechanism by which the mRNA interacts with the ribosome to bring about a frameshift remains a mystery. Somehow, the tRNAs in the ribosomal A and P sites simultaneously slip back one base on the mRNA before (5) or after (3) peptide bond formation, and translation resumes in the new (−1) reading frame. This requires pausing of the ribosome induced by the adjacent pseudoknot in the mRNA (10, 11). A long-standing enigma has been the observations that only certain pseudoknots facilitate frameshifting, whereas other very similar structures of comparable stability do not cause frameshifting (12–14), even though they induce pausing (15). Other elements, such as downstream stop codons and the RNA sequences surrounding the shifty site, can influence the effectiveness of these signals (16). Mutations in ribosomal proteins (17), translation factors (18), and nonsense-mediated decay factors (19) can alter frameshift efficiency. Their precise roles are unknown.

The true contributions of the above cis and trans acting components to frameshifting in the context of the virus in its host can be difficult to assess, as most studies rely on reporter plasmids using small portions of viral sequence. Yet, viral gene expression and replication, can be controlled by long-distance interactions on viral RNAs (20, 21). In poliovirus (22) and bacteriophage Qβ (23) RNAs, replicase binds far upstream of the 3′ end, shutting off translation, and is delivered to the 3′ end, where replication initiates, by protein–RNA interactions in poliovirus (20) or long-distance base pairing in Qβ RNA (24). These long-distance interactions allow these RNA viruses to switch between replication and translation, events that are incompatible on the same RNA. How other viruses regulate this switch is poorly understood. *Barley yellow dwarf virus* (BYDV) uses multiple long-distance interactions to regulate cap-independent translation initiation (25), ribosomal frameshifting (26), and leaky termination (27). The cap-independent translation element (3′ TE) in the 3′ untranslated region (UTR) must form base pairs with a stem loop in the 5′ UTR to facilitate translation of this naturally uncapped mRNA (25). The effects of such interactions would be missed in studies that examine the translation signals out of their natural sequence context.

ORF 2, which codes for the RNA-dependent RNA polymerase (RdRp) of BYDV, is expressed via −1 frameshift from the overlapping ORF 1 (Fig. 1*A*). Frameshifting takes place at the shifty site, G GGU UUU, yielding the 99-kDa fusion product (P1-2) of the 39-kDa ORF 1 product (P1) and 60-kDa ORF 2 product (28, 29). Beginning 6 nt downstream of the shifty heptanucleotide, a large bulged stem-loop structure is predicted (29). An additional sequence located 4 kilobases downstream in the 3′ UTR of BYDV genomic RNA is necessary for frameshifting in wheat germ extract (WGE) (26). This includes a 50-base essential ''core'' element (nt 5,050–5,100) and an adjacent ''enhancer'' region (BYDV nt 5,101–5,283) that, when deleted, causes a 50% decrease in frameshifting (26). Here, we use a dual luciferase reporter system (30) to map the distant downstream element at higher resolution *in vivo* and *in vitro*. We find that an intramolecular association of this element with the bulge of the stem loop at the frameshift site via base pairing is required. We propose a role for this remarkable new type of

This paper was submitted directly (Track II) to the PNAS office.

Abbreviations: BYDV, *Barley yellow dwarf virus*; ADSL, adjacent downstream stem loop; LDFE, long-distance frameshift element; WGE, wheat germ extract; UTR, untranslated region; RdRp, RNA-dependent RNA polymerase.

*Present address: Pioneer Hi-Bred International, 7300 SW 62nd Avenue, Johnston, IA 50131.

†To whom reprint requests should be addressed. E-mail: wamiller@iastate.edu.

BIOCHEMISTRY

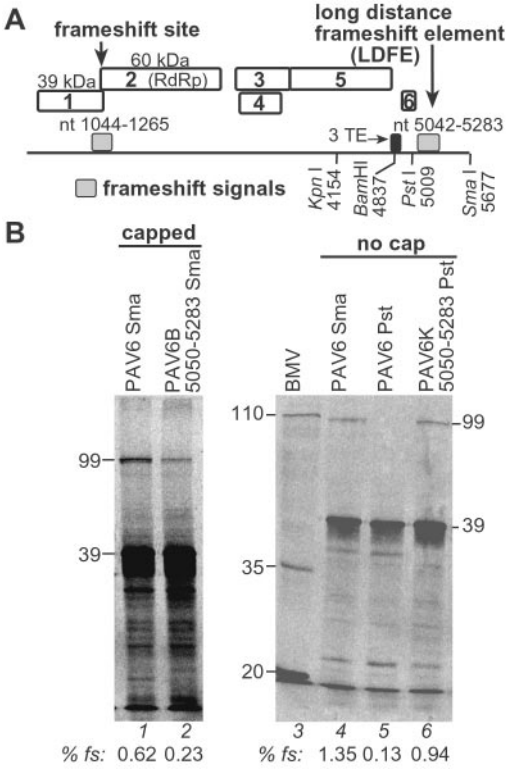

Fig. 1. Mapping of long-distance frameshift element *in vitro*. (*A*) BYDV genome organization. Frameshift elements are shown as gray boxes; numbering indicates base positions (nt) in BYDV genome. (*B*) Wheat germ translation products of viral transcripts. PAGE and quantification of frameshifting are described in *Materials and Methods*. Frameshift efficiencies (% fs) are shown under each lane. Translation of capped transcripts from wild-type *Sma*I-linearized pPAV6 (lane 1), and mutant containing only bases 5,050–5,283 downstream of the *Bam*HI$_{4837}$ site (lane 2). Lanes 4–6, translation of uncapped transcripts from *Sma*I or *Pst*I-cut pPAV6 or from *Pst*I-cut pPAV6K5050–5283 that contains bases 5,050–5,283 in the *Kpn*I$_{4154}$ site. Mobilities of the products of BYDV ORF1 (39 kDa), ORF 1 + 2 (99 kDa), respectively, and *Brome mosaic virus* (BMV) RNA translation products (lane 3) are marked.

frameshift signal, along with the long-distance cap-independent translation base pairing, in an elegant mechanism for regulating translation and replication.

Materials and Methods

Template Construction for Frameshift Assay. The dual luciferase vector was constructed by cloning the Renilla (jellyfish) luciferase gene (rLUC) and the BYDV frameshift site into p5′UTR-fLUC-TE869-(A)60 (31). This vector contains the 5′UTR of BYDV (nt 1–152), a *Photonius* (firefly) luciferase gene (fLUC), the 3′UTR (nt 4809–5677), and a 60-base poly(A) tail. The rLUC gene was generated by PCR with *Bss*HII and *Kpn*I restriction sites from the p2luc vector (30) and ligated in between the BYDV 5′ UTR and the *Kpn*I site in the 5′ end of fLUC. Sequence spanning the BYDV frameshift site (nt 1,039–1,262) was then ligated in between the rLUC and fLUC genes by using the *Apa*I/*Sac*I site so that a −1 frameshift is necessary for translation of the downstream fLUC ORF. The 1,039–1,262-nt region was generated by PCR from three different plasmids: pPAV6 with the wild-type shifty site (G GGU UUU); pM4, which differs only by an insertion in the shifty site (G GGU UUC U), placing fLUC in-frame with the upstream rLUC gene; and pSHSIL in which the shifty site was destroyed (C GGC UUC; ref. 26). All other mutations in the frameshift region were generated by incorporating the nucleotide changes into the forward or reverse primer. All mutants were cloned into all three vectors: the wild-type, the in-frame, and the disrupted shifty site.

The 3′ UTR mutations were generated by using full-length BYDV genomic clone pPAV6 as template (28). Deletions were generated via the ExSite PCR-based site-directed mutagenesis kit (Stratagene). The forward and reverse primers contain an *Nco*I site at either the 3′ or the 5′ end of the deletion desired. The PCR reaction was cleaved with *Nco*I, and then the two ends were ligated. The region between *Bam*HI$_{4837}$ and *Sma*I$_{5677}$ sites was sequenced before ligation into the dual luciferase vector by using these sites. Point mutations were introduced by using the Quick Change method (Stratagene). Forward and reverse primers containing the desired mutations were used on pPAV6 template. Mutations were sequenced and cloned into the dual luciferase vector as described above.

Insertion mutants were generated by amplifying the BYDV sequence using a forward primer with *Bam*HI and a reverse primer with *Sma*I sites at their 5′ termini to produce the region of interest from pPAV6. For the insertion mutants into the *Kpn*I site, the forward and reverse primers both contained a *Kpn*I site. These fragments were generated by using PCR, gel purified, and ligated into pPAV6 that was digested with the same enzymes.

***In Vitro* Transcription.** Uncapped and capped BYDV-derived RNAs were transcribed by using the Megascript and mMessage mMachine kits (Ambion, Austin, TX), respectively, from pPAV6 or its derivatives cleaved with *Sma*I (3′ end of BYDV) or other indicated restriction enzymes. Dual luciferase vector transcripts were synthesized in the same manner but from plasmid cleaved with *Nhe*I, which retained the A_{60} tail. *Pst*I-linearized DNA was filled in with Klenow polymerase fragment before transcription.

***In Vitro* Translation.** *In vitro* translation was performed in WGE (Promega) as described previously (26). Bands were quantitated by using a STORM PhosphorImager and IMAGEQUANT software (Molecular Dynamics). To correct for the number of methionines in each product, the frameshift efficiency for the BYDV constructs was calculated as [(99-kDa counts/28 Met)/(99-kDa counts/28 Met + 30-kDa counts/10 Met)] × 100, and the dual luciferase constructs were [(100-kDa counts/22 Met)/(100-kDa counts/22 Met + 40-kDa counts/9 Met)] × 100.

Translation and Replication in Protoplasts. For luciferase assays, oat protoplasts were prepared from suspension cells, electroporated with 15 μg of RNA transcripts, and harvested after 4 to 6 h (25, 26). Cells were lysed in 100 μl of passive lysis buffer by shaking for 15 min at room temperature and spun to remove debris. Ten-microliter aliquots of supernatant were assayed by using the Stop and Glo dual luciferase kit (Promega). All mutants were tested in triplicate in the wild-type, in-frame, and out-of-frame vectors. The percent frameshifting was calculated by determining the fLUC/rLUC ratio for all constructs and then dividing this number by the ratio for the positive control (the same mutation cloned into the dual luciferase vector with the in-frame, GGGUUUCU shifty site). The results were compared with the negative control (dual luciferase vector with the nonshifting CGGCUUC sequence in the shifty site), which was around 20% of the wild-type frameshift signal. The percent frameshifting for the mutants was then reported as that compared with the wild-type control run on the same day. For RNA replication assays, protoplasts were electroporated with BYDV transcripts as above. After 24 h, total RNA was extracted and analyzed by Northern blot hybridization (26).

Results

Minimal Frameshift Enhancer Element Established *in Vitro*. Previously, we showed that deletions within bases 5,050–5,283 reduced or abolished frameshifting *in vitro*, whereas individual

deletions upstream or downstream did not (26). Here, we determine whether bases 5,050–5,283 are sufficient to stimulate frameshifting at the level observed with full-length RNA and whether the positioning of this element influences the frameshifting efficiency. To test this, the sequences from the *Bam*HI$_{4837}$ site to nt 5050 and from nt 5283 to the 3′ end were deleted (Fig. 1*B*, PAV6B5050–5283). This construct lacks the 3′ TE necessary for cap-independent translation, so it and the wild-type control RNA (PAV6) were capped for efficient translation in WGE. Presence of the 5′ cap reduced wild-type frameshift efficiency by 50% (Fig. 1*B*, compare lanes 1 and 4), as observed previously (26). PAV6B5050–5283 RNA induced about one-third as much frameshifting as wild-type RNA (Fig. 1*B*, lanes 1 and 2). Because BYDV sequences deleted from this construct were shown separately to be unnecessary for frameshifting (26), these results suggest that the location of the frameshift element at the very 3′ end reduces its activity.

To determine whether it was simply proximity to the 3′ end that reduced frameshifting, the 5,050–5,283 sequence was inserted in the unique *Kpn*I$_{4154}$ site in the expendable ORF 5 of the full-length BYDV transcript (Fig. 1*B*, PAV6K5050–5283). The transcript was truncated at the *Pst*I$_{5009}$ site (nt 5,009) leaving 850 nt of viral sequence (unnecessary for frameshifting; ref. 26) downstream of the ectopic 5,050–5,283 insertion in the *Kpn*I$_{4154}$ site. This truncated RNA frameshifted about as efficiently as wild type (Fig. 1*B*, lane 6). As a control, *Pst*I truncation was shown to abolish frameshifting in the wild-type PAV6 RNA (Fig. 1*B*, lane 5). Therefore, the region between 5,050–5,283 contains the complete long-distance frameshift element (LDFE) necessary for frameshifting *in vitro*; however, it is less effective when located at the very 3′ end.

Sequences Upstream and Downstream of the Shifty Site Are Necessary for Frameshifting *in Vivo*. For high resolution mapping of the frameshift signals *in vivo* and *in vitro*, we used a dual luciferase reporter that allows precise frameshift measurement. The dual luciferase reporter contains a Renilla luciferase (rLUC) gene in the zero frame, followed by a firefly luciferase (fLUC) ORF in the −1 frame, with the candidate frameshift sequence inserted between two reporters (30). The fLUC/rLUC ratio reveals the frameshift efficiency (Fig. 2*A*). We inserted the shifty site, the proposed adjacent downstream stem loop (ADSL), and substantial adjacent viral sequence upstream of the shifty site between the rLUC and fLUC ORFs (nt 1,044–1,250). Two additional regions of BYDV sequence, the 5′ UTR (nt 1–152) and the 3′ UTR (nt 4,908–5,677), were included so that the resulting transcript, DL-PAV206, had all of the UTR sequences necessary for cap- and poly(A)-independent translation (25). The missing viral RNA, bases 152–1,046 and 1,648–4,919, do not play a role in translation initiation or frameshifting *in vitro* (26, 32).

In oat protoplasts, DL-PAV206 RNA frameshifted with 1.1% efficiency, consistent with WGE results for full-length viral RNA (Fig. 2*A*). As expected, deletion of the ADSL reduced frameshifting to near background levels (Fig. 2*A*, DL-PAVSL). Following translation in WGE, the rLUC-fLUC frameshift product of DL-PAV206 RNA was clearly visible compared with the SHSIL transcript with the disrupted shifty site (Fig. 2*B*, lanes 1 and 3). Deletions upstream of the shifty site between nt 1,044–1,139 reduced frameshifting by about half *in vivo* (Fig. 2*A*, DL-PAV111, 129, and 167), but not *in vitro* (data not shown). Although this result is not predicted from other known frameshift signals, previous experiments with BYDV genome deletions indicated that upstream sequence might be important for frameshifting *in vitro* (32). Thus, the dual luciferase vector containing BYDV nt 1,044–1,250 between the rLUC and fLUC ORFs responds to mutations as expected and is a cogent model for viral RNA frameshifting.

A series of deletion mutants within the region spanning nt

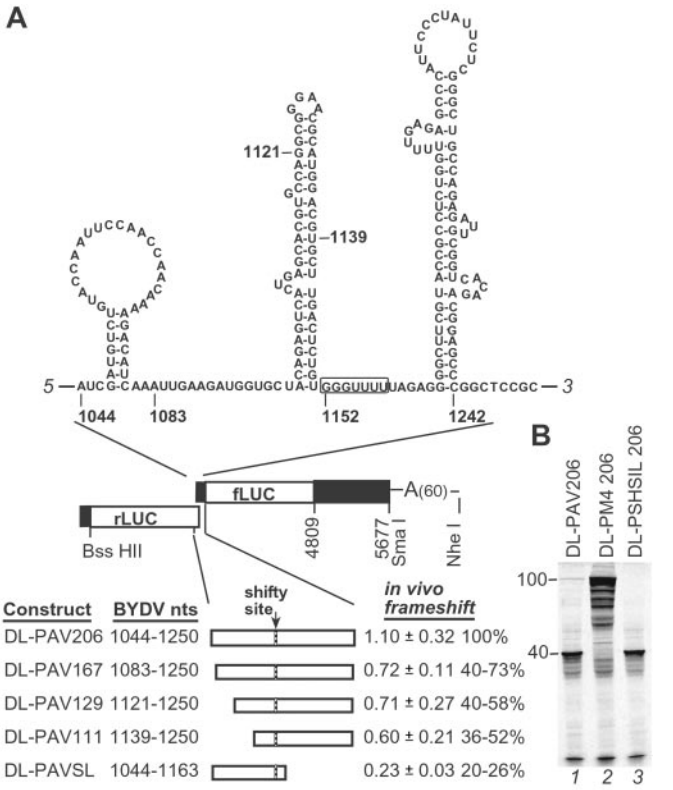

Fig. 2. Frameshifting in the dual luciferase vector. (*A*) Map of vector showing predicted BYDV RNA secondary structure around the shifty site inserted between the two LUC ORFs. The BYDV 3′ UTR is inserted after fLUC. BYDV sequences are represented by black boxes. Frameshift rates (±SD) in oat protoplasts (*in vivo*) were calculated as described in *Materials and Methods*. The percentage of frameshifting is calculated by using the DL-PAV206 control value for that individual assay. All constructs were tested in triplicate at least twice except for DL-PAV-SL, which was tested once. (*B*) *In vitro* translation products of dual luciferase constructs with different shifty site sequences. The rLUC (40 kDa) and rLUC-fLUC (100 kDa) products are marked. DL-PSHSIL206 has a disrupted shifty site (see *Materials and Methods*). Both LUC ORFs are fused in the same frame in DL-PM4 206.

5,016–5,426 was constructed in the dual luciferase vector to more precisely map the LDFE *in vivo* (Fig. 3). Deletion of nt 5,047–5,099 reduced frameshifting to background levels (about 0.2% frameshifting or 20% of that obtained with the full-length UTR). Deletions in nt 5,168–5,279 gave 30–50% of wild-type frameshifting. The sequence between nt 5,091–5,168 is not necessary for frameshifting. Thus, the essential core and enhancer sequences are two separate elements. Furthermore, *in vivo*, additional sequence was required beyond what is necessary for frameshift enhancer activity *in vitro*. Sequence between 5,319 and 5,355 was necessary for full frameshifting *in vivo* (Fig. 3), but no sequence downstream of nt 5,283 was necessary *in vitro* (26).

Base Pairing Between the Adjacent Bulged Stem Loop and the Long-Distance Frameshift Element Is Essential for Frameshifting. We next investigated how the ADSL and the distant LDFE both participate in frameshifting. Within the core LDFE, nucleotides 5,057–5,075 are conserved among all BYDV isolates (26) and are predicted by MFOLD (33) to form a stem-loop structure. Six contiguous bases (underlined) in loop $_{5063}$A<u>UCUGUG</u>$_{5069}$, can potentially base pair to six conserved bases in the ADSL of the frameshift site $_{1229}$CACAGA$_{1234}$ (Fig. 4*A*). Five of these ADSL bases are in a predicted bulge. Formation of six base pairs between the LDFE loop and the ADSL bulge requires disruption

BIOCHEMISTRY

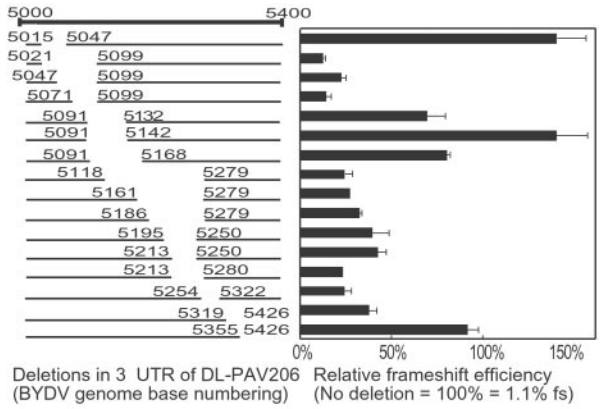

Fig. 3. Frameshifting in oat protoplasts of BYDV 3′ end deletion mutants. All deletion constructs are in the DL-PAV206 *Sma*I-linearized background. Results are graphed as the % of the frameshift efficiency (fs) of DL-PAV206 (fs = 1.10%; Fig. 2*A*), which contains the full-length 3′ UTR (nt 4,809–5,677). Each sample was tested in triplicate two independent times; error bars represent the SD.

of one adjacent base pair (U_{1172}:A_{1234}) in the ADSL. The potential for this long-distance base pairing is conserved in all BYDV isolates and in the only other sequenced BYDV-like virus, *Soybean dwarf virus* (SbDV). The predicted LDFE of SbDV has the potential to form seven base pairs with the bulge in the ADSL, but the LDFE "stem" is very weak (Fig. 4*A*, SbDV).

We tested the existence and function of this long-distance base pairing by monitoring translation of transcripts with altered sequences within this region. The potential base pairing was disrupted and restored by changing the sequence of one or both of the predicted strands of the long-distance interaction. Mutating all six bases to the complementary sequence (DL-BL1230 or DL-SL5066), or altering just the central two bases (DL-PT1230 or DL-PT5066) in either strand, dramatically reduced frameshifting *in vivo* and *in vitro* (Fig. 4*B*). When the mutations in each region were combined in the double mutants to restore base pairing, frameshifting increased substantially. Thus, the long-distance base pairing, and not the primary sequence, is the important component for frameshift stimulation by the LDFE stem loop and ADSL bulge.

Base Pairing Between the Adjacent Downstream Stem Loop and the Long-Distance Frameshift Element Is Essential for Viral RNA Replication. To test the role of the long-distance base pairing in the actual context of the replicating virus, we assayed the ability of full-length infectious BYDV RNA with altered frameshift elements to replicate in oat protoplasts. The frameshift is essential for BYDV replication because frameshifting is necessary for translation of the viral RdRp (26, 32). One constraint for mutating the ADSL RNA sequence is that the resulting alteration in the amino acid sequence of the RdRp could reduce its activity, independent of frameshift efficiency (32). To minimize this possibility, replication was tested only for the ADSL constructs with two-base mutations (PAV6 PT1230, PAV6 PT1230/PT5066). The PT1230 mutation introduces a relatively conservative change of serine to threonine in the RdRp, whereas the PT5066 mutation is in the UTR. These mutations had the same effects on frameshifting of full-length viral genomic RNA as on the reporter constructs *in vitro* (Fig. 4*C*). In protoplasts, the PAV6-derived transcripts with either of the two-base mutations did not replicate, as revealed by Northern blot analysis of viral RNA accumulation at 24 hpi (Fig. 4*D*, PAV PT1230 and PAV PT5066). In contrast, the double mutant, which restores the

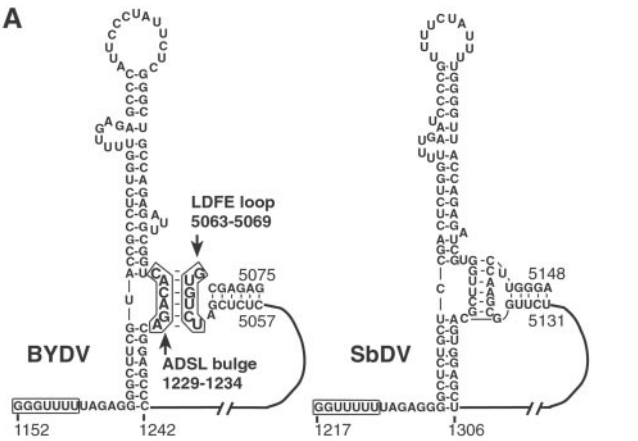

B

transcript	ADSL bulge	LDFE loop	long distance base-pairing	frameshift efficiency in vitro	frameshift efficiency in vivo
DL-PAV206 (wt)	CACAGA	UCUGUG	+	0.35 (100%)	1.10 (100%)
DL-BL1230	**GUGUCU**	UCUGUG	-	0.09 (26%)	0.12 (11%)
DL-SL5066	CACAGA	**AGACAC**	-	0.06 (17%)	0.14 (13%)
DL-BL1230/SL5066	**GUGUCU**	**AGACAC**	+	0.24 (69%)	0.63 (57%)
DL-PT1230	CA**GU**GA	UCUGUG	-	0.04 (11%)	0.12 (11%)
DL-PT5066	CACAGA	UC**AC**UG	-	0.02 (6%)	0.15 (14%)
DL-PT1230/PT5066	CA**GU**GA	UC**AC**UG	+	0.24 (69%)	0.76 (69%)

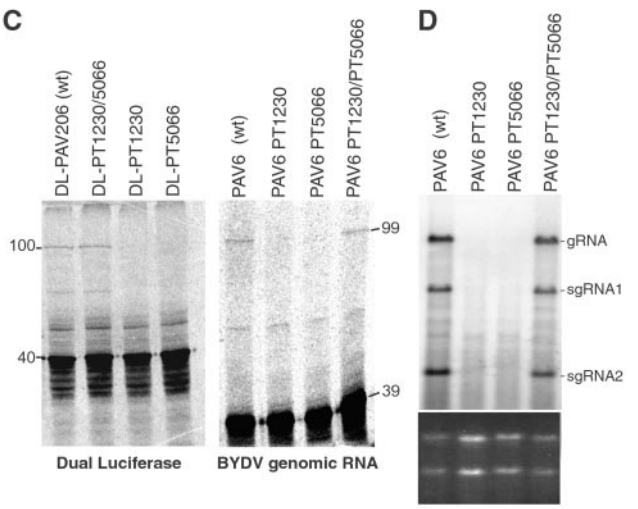

Fig. 4. Frameshifting and replication of BYDV mutants that destroy and restore the long-distance base pairing. (*A*) Predicted secondary structures (MFOLD) of BYDV and the related SbDV RNAs showing the base-pairing interaction (boxed in BYDV structure) of the long-distance frameshift element (LDFE) with the bulge in the adjacent downstream stem loop (ADSL bulge). (*B*) Frameshift efficiencies of dual luciferase constructs with mutations in ADSL bulge and/or LDFE that disrupt and restore potential base pairing. Frameshift efficiencies are averages from three independent experiments. The nucleotide sequence for the two regions for each mutant is shown with altered bases in bold. (*C*) PAGE of wheat germ translation products of BYDV dual luciferase (100-kDa frameshift product) and of full-length viral (PAV6) constructs containing the same sets of two-base mutations in the ADSL and/or LDFE. (*D*) Northern blot hybridization of RNA from oat protoplasts inoculated with the same wild-type and mutant PAV6 transcripts used in *C*. BYDV genomic (gRNA) and subgenomic RNAs (sgRNA) produced during virus replication are marked. (*Lower*) Ethidium bromide staining of gel used for the above blot as a control for gel loading. This experiment was repeated three times with the same results.

base-pairing interaction, replicated at wild-type levels (Fig. 4*D*, PAV PT1230/PT5066). These results demonstrate that the long-distance base pairing is required in the natural viral RNA

replication process, as predicted by its essential role for frameshifting.

Discussion

The Measured Frameshift Efficiency of BYDV Is Low but Significant. The dual luciferase vector allows accurate measurement of very small changes in frameshifting efficiency, well below 1% in plant cells. Low but significant levels were also detectable *in vitro* with radiolabeled translation products (Figs. 2*B* and 4). Western blots indicated ratios of postshift to preshift (P1–2:P1) proteins in infected cells of at least 6% (26), suggesting a higher frameshift efficiency in a natural infection. Frameshifting may be reduced in the dual reporter system because it may lack important viral sequence needed only *in vivo*. Indeed, we found that more sequence (nt 1,044–1,138 and 5,320–5,355) had a positive effect *in vivo* than *in vitro* (Figs. 2*A* and 3). This resembles cap-independent translation, which also requires more sequence in the 3′ UTR *in vivo* than *in vitro* (31), perhaps because of the presence of host mRNAs providing more competition for the translation machinery. The lower frameshifting by the dual reporter system may be because of parameters that are not controlled directly by frameshift elements, such as initiation rate (11, 26, 34), or the sequence context of the stimulatory elements (16, 26). The above caveats aside, it is clear that the long-distance base pairing is essential for −1 ribosomal frameshifting in all assays and, most importantly, in the context of replicating viral RNA. The latter was demonstrated by the complete ablation of BYDV replication by base changes in either the ADSL or the LDFE, and the complete restoration of replication in the double compensatory mutant (Fig. 4*D*).

The frameshift enhancement by the sequence upstream of the shifty site (nt 1,044–1,139) in the dual luciferase reporter system (Fig. 2*A*) was unexpected. However, the eight bases immediately upstream of the HIV-1 and HTLV-2 shifty sites are known to affect frameshifting (16). The stem loop predicted by MFOLD (33) immediately upstream of the shifty site is conserved in all members of the *Luteovirus* and *Dianthovirus* genera. These upstream stem loop(s) may slow the ribosome in advance of the shifty site to enhance frameshifting. Alternatively, they may serve as "insulators" to prevent improper folding of the shifty site or ADSL with upstream sequences.

Interestingly, a bulged stem loop very similar to the ADSL of BYDV RNA stimulates *Red clover necrotic mosaic dianthovirus* (RCNMV) RNA frameshifting, in the absence of its viral 3′ UTR, in rabbit reticulocyte lysates (8) and in dual luciferase reporter transcripts in WGE (J.K.B., unpublished results). However, whether the RCNMV 3′ UTR further stimulates frameshifting remains to be tested. By analogy, in HIV RNA, an ADSL was thought to be sufficient to stimulate frameshifting (35), but for full frameshifting, the ADSL must interact with nearby downstream sequence to form a novel pseudoknot with a base triplex in the stem (9). Potential for long-distance base pairing between a 3′ UTR element and the bulged stem loop adjacent to the frameshift site is conserved in SbDV (Fig. 4*A*) and in genus *Dianthovirus*, including RCNMV (not shown). The predicted base pairing of the SbDV putative LDFE to the ADSL bulge is long (7 bp) and GC-rich, but the predicted distant "stem" in SbDV is so weak (G:U-rich) that it may not exist (Fig. 4*A*). Nevertheless, this phylogenetic conservation supports a functional role for the long-distance base pairing.

The Long-Distance Loop:Bulge Base Pairing Is a Previously Uncharacterized Frameshift Structure. Gene 10 of bacteriophage T7 provides another example of −1 frameshifting stimulated by an element beyond the immediate vicinity of the frameshift site. It requires a sequence located 200 bases downstream of the shifty site that is predicted to form a stem loop (36). However, it is the sequence in this region and not predicted secondary structure that stimulates frameshifting. Perhaps the structures most similar to that of BYDV are found in Rous sarcoma virus (37) and gill-associated virus (38) RNAs. As in BYDV RNA, these structures consist of a long, bulged ADSL and a downstream region base-paired to a bulge in the ADSL. Unlike BYDV, the downstream element is not a stem loop; it is only 12–42 nt downstream of the ADSL, and the bulge to which its base pairs is on the 5′ rather than the 3′ side of the ADSL. A example of a different kind of recoding that is facilitated by a sequence in the 3′ UTR is the incorporation of the amino acid selenocysteine at UGA codons (39). However, that interaction uses specialized translation elongation factors (39) rather than long-distance base pairing. Thus, the bulge-loop:stem-loop interaction in BYDV RNA is a different class of long-distance recoding element.

How RNA structures stimulate ribosomes to change frame is unknown, but one of their key roles in frameshifting is to pause the ribosome over the shifty site (11, 15). The properties that determine whether a structure stimulates frameshifting are unclear. A comparison of the high-resolution structures determined for the MMTV (40), BWYV (41), and other frameshift pseudoknots reveals no tell-tale structural features (4). It has been proposed that frameshift efficiency is determined by the ability of the pseudoknot to resist the ribosomal helicase activity

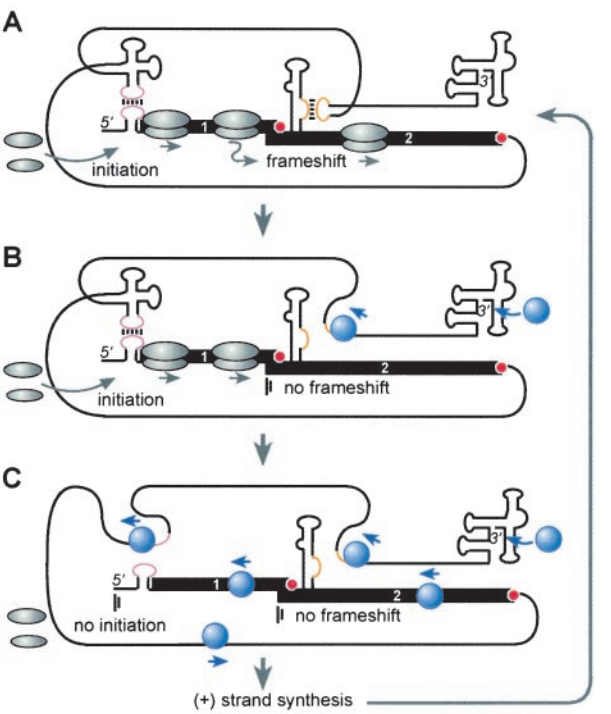

Fig. 5. RNA traffic signal hypothesis for regulation of BYDV translation and replication. Black line indicates BYDV genomic RNA showing relevant secondary structural elements with key regions in color (not to scale). Black boxes indicate ORFs 1 and 2. For simplicity, other ORFs, nascent proteins, and (−) strand RNA are not shown. (*A*) Base pairing between the 3′ TE and 5′ UTR (magenta) (25) and between the LDFE and ADSL (gold) allow ribosomes (gray ovals) to translate ORF 1 and ORF 2. (*B*) As the viral RdRp molecules (blue spheres) accumulate, they initiate (−) strand synthesis at the 3′-terminal structure (46). They proceed upstream along the template and melt out the ADSL:LDFE base pairing. This blocks frameshifting (vertical bars), clearing ORF 2 of ribosomes, briefly allowing translation of ORF1 only. (*C*) Next, the RdRp reaches the 3′ TE and disrupts the 3′TE:5′ UTR base pairing, preventing translation initiation. This clears ORF1 and the entire RNA of ribosomes, allowing the RdRps to continue to the 5′ end. Subsequent rounds of replication would cause (+) strand RNA to accumulate in excess of RdRp molecules, returning the process to *A* as shown.

during translation elongation (4, 9, 14). Yusupova *et al.* (42) propose that three ribosomal proteins surrounding the mRNA entry site into the 80S complex bind helical regions on the mRNA and separate the strands as the mRNA enters the ribosome. Therefore, the authors speculated that frameshift-stimulatory structures preclude efficient interactions with these helix-unwinding proteins. The bulge-loop:stem-loop helix formed by the long-distance interaction in BYDV RNA may coaxially stack with (one of) the flanking helices in the ADSL, stabilizing the long-distance base pairing, and forming a stable, kinked, helical structure that proves awkward for the ribosome to unwind. This could facilitate frameshifting by the above mRNA–ribosome interaction.

A Potential Translation–Replication Switch. The location of both the cap-independent translation initiation element and the frameshift element far downstream of the translated genes provides advantages for the virus. Owing to their location in the UTR, they are unfettered by protein coding constraints. Second, this location would prevent unproductive translation of 3′ truncated mRNA that is either partially degraded or not fully synthesized. Most interestingly, a requirement for base pairing of 3′ UTR elements to upstream sequences for translation (25) may provide a novel mechanism to prevent collisions between ribosomes and the replicase. Translating ribosomes block replicase molecules moving in the opposite direction on the same template RNA (22, 43). Poliovirus avoids this event as its replicase first binds the viral 5′ UTR to shut off translation and is then delivered to the 3′ end via protein–protein interactions to initiate (−) strand synthesis (20). According to our model (Fig. 5), early in infection newly translated replicase binds the 3′ end of viral RNA and proceeds through the 3′ UTR toward the 5′ end as it synthesizes (−) strand. Upon reaching the LDFE and the 3′ TE, replicase disrupts both sets of long-distance base pairing, thus blocking frameshifting and translation initiation. These events would clear ORF 2 and then ORF 1 of ribosomes, allowing replicase to complete full-length (−) strand synthesis from a ribosome-free (+) strand. As replicase subsequently produces (+) strand genomic RNA copies from the (−) strand template, eventually (+) strands would outnumber replicase molecules and be free to form the long-distance base-pairing interactions necessary for translation initiation and frameshifting, and the cycle would repeat. This model provides an elegant means to allow simultaneous replication and translation while avoiding nonproductive collisions between replicase and ribosome. This model is consistent with our unexplained observation that capped BYDV transcripts are far less infectious than uncapped transcripts (44). Presence of a 5′ cap would favor continuous translation, preventng the replicase from copying ribosome-laden viral RNA. This mechanism may serve instead of, or in addition to, subcellular vesicles that may separate the sites of translation and replication of some viruses, such as BMV (45). The fact that frameshifting would be disrupted slightly before initiation by the replicase hints that expression of the RdRp (frameshift product of ORFs 1 + 2) may be regulated differently from the product of ORF 1 alone.

We thank Gloria Culver and Ian Brierley for advice on the manuscript and Guido Grentzmann and John Atkins for the dual luciferase reporter plasmid. This research was funded by National Institutes of Health Fellowship 1 F32 AI10445-01 (to J.K.B.) and by National Science Foundation Grant MCB-9974590 and U.S. Department of Agriculture/National Research Initiative (2001-35319-10011) (to W.A.M.). This paper is no. J-19792 of the Iowa Agriculture and Home Economics Experiment Station, Project 6542.

1. Gesteland, R. F. & Atkins, J. F. (1996) *Annu. Rev. Biochem.* **65,** 741–768.
2. Brierley, I. & Pennell, S. (2001) in *The Ribosome: Cold Spring Harbor Symposia on Quantitative Biology, LXVI* (Cold Spring Harbor Lab. Press, Plainview, NY), Vol. 66, pp. 233–248.
3. Farabaugh, P. J. (1996) *Microbiol. Rev.* **60,** 103–134.
4. Giedroc, D. P., Theimer, C. A. & Nixon, P. L. (2000) *J. Mol. Biol.* **298,** 167–185.
5. Jacks, T., Madhani, H. D., Masiarz, F. R. & Varmus, H. E. (1988) *Cell* **55,** 447–458.
6. Brierley, I., Digard, P. & Inglis, S. C. (1989) *Cell* **57,** 537–547.
7. Parkin, N. T., Chamorro, M. & Varmus, H. E. (1992) *J. Virol.* **66,** 5147–5151.
8. Kim, K. H. & Lommel, S. A. (1998) *Virology* **250,** 50–59.
9. Dinman, J. D., Richter, S., Plant, E. P., Taylor, R. C., Hammell, A. B. & Rana, T. M. (2002) *Proc. Natl. Acad. Sci. USA* **99,** 5331–5336.
10. Tzeng, T. H., Tu, C. L. & Bruenn, J. A. (1992) *J. Virol.* **66,** 999–1006.
11. Lopinski, J. D., Dinman, J. D. & Bruenn, J. A. (2000) *Mol. Cell. Biol.* **20,** 1095–1103.
12. Kim, Y. G., Su, L., Maas, S., O'Neill, A. & Rich, A. (1999) *Proc. Natl. Acad. Sci. USA* **96,** 14234–14239.
13. Liphardt, J., Napthine, S., Kontos, H. & Brierley, I. (1999) *J. Mol. Biol.* **288,** 321–335.
14. Chen, X., Kang, H., Shen, L. X., Chamorro, M., Varmus, H. E. & Tinoco, I. (1996) *J. Mol. Biol.* **260,** 479–483.
15. Kontos, H., Napthine, S. & Brierley, I. (2001) *Mol. Cell. Biol.* **21,** 8657–8670.
16. Kim, Y. G., Maas, S. & Rich, A. (2001) *Nucleic Acids Res.* **29,** 1125–1131.
17. Peltz, S. W., Hammell, A. B., Cui, Y., Yasenchak, J., Puljanowski, L. & Dinman, J. D. (1999) *Mol. Cell. Biol.* **19,** 384–391.
18. Cui, Y., Dinman, J. D., Kinzy, T. G. & Peltz, S. W. (1998) *Mol. Cell. Biol.* **18,** 1506–1516.
19. Dinman, J., Ruiz-Echevarria, M., Wang, W. & Peltz, S. (2000) *RNA* **6,** 1685–1686.
20. Herold, J. & Andino, R. (2001) *Mol. Cell* **7,** 581–591.
21. Klovins, J. & van Duin, J. (1999) *J. Mol. Biol.* **294,** 875–884.
22. Gamarnik, A. V. & Andino, R. (1998) *Genes Dev.* **12,** 2293–2304.
23. Brown, D. & Gold, L. (1996) *Proc. Natl. Acad. Sci. USA* **93,** 11558–11562.
24. Klovins, J., Berzins, V. & van Duin, J. (1998) *RNA* **4,** 948–957.
25. Guo, L., Allen, E. & Miller, W. A. (2001) *Mol. Cell* **7,** 1103–1109.
26. Paul, C. P., Barry, J. K., Dinesh-Kumar, S. P., Brault, V. & Miller, W. A. (2001) *J. Mol. Biol.* **310,** 987–999.
27. Brown, C. M., Dinesh-Kumar, S. P. & Miller, W. A. (1996) *J. Virol.* **70,** 5884–5892.
28. Di, R., Dinesh-Kumar, S. P. & Miller, W. A. (1993) *Mol. Plant–Microbe Interact.* **6,** 444–452.
29. Brault, V. & Miller, W. A. (1992) *Proc. Natl. Acad. Sci. USA* **89,** 2262–2266.
30. Grentzmann, G., Ingram, J. A., Kelly, P. J., Gesteland, R. F. & Atkins, J. F. (1998) *RNA* **4,** 479–486.
31. Guo, L., Allen, E. & Miller, W. A. (2000) *RNA* **6,** 1808–1820.
32. Mohan, B. R., Dinesh-Kumar, S. P. & Miller, W. A. (1995) *Virology* **212,** 186–195.
33. Mathews, D. H., Sabina, J., Zuker, M. & Turner, D. H. (1999) *J. Mol. Biol.* **288,** 911–940.
34. Honigman, A., Falk, H., Mador, N., Rosental, T. & Panet, A. (1995) *Virology* **208,** 312–318.
35. Kollmus, H., Honigman, A., Panet, A. & Hauser, H. (1994) *J. Virol.* **68,** 6087–6091.
36. Condron, B. G., Gesteland, R. F. & Atkins, J. F. (1991) *Nucleic Acids Res.* **19,** 5607–5612.
37. Marczinke, B., Fisher, R., Vidakovic, M., Bloys, A. J. & Brierley, I. (1998) *J. Mol. Biol.* **284,** 205–225.
38. Cowley, J. A., Dimmock, C. M., Spann, K. M. & Walker, P. J. (2000) *J. Gen. Virol.* **81,** 1473–1484.
39. Tujebajeva, R. M., Copeland, P. R., Xu, X. M., Carlson, B. A., Harney, J. W., Driscoll, D. M., Hatfield, D. L. & Berry, M. J. (2000) *EMBO Rep.* **1,** 158–163.
40. Shen, L. X. & Tinoco, I. J. (1995) *J. Mol. Biol.* **247,** 963–978.
41. Su, L., Chen, L., Egli, M., Berger, J. M. & Rich, A. (1999) *Nat. Struct. Biol.* **6,** 285–292.
42. Yusupova, G. Z., Yusupov, M. M., Cate, J. H. & Noller, H. F. (2001) *Cell* **106,** 233–241.
43. Barton, D. J., Morasco, B. J. & Flanegan, J. B. (1999) *J. Virol.* **73,** 10104–10112.
44. Allen, E., Wang, S. & Miller, W. A. (1999) *Virology* **253,** 139–144.
45. Schwartz, M., Chen, J., Janda, M., Sullivan, M., den Boon, J. & Ahlquist, P. (2002) *Mol. Cell* **9,** 505–514.
46. Koev, G., Liu, S., Beckett, R. & Miller, W. A. (2002) *Virology* **292,** 114–126.